Low-temperature spectroscopic studies of single molecules in 3-D and on 2-D hosts

Smit, R.

3

THE PHOSPHORESCENCE OF PERYLENE

In this chapter, I will show how we used the dibenzothiophene host matrix to enhance the phosphorescence signal from embedded perylene-d12 molecules. We excited the host molecules with UV light from a mercury light source and we observed a strong phosphorescence signal due to strong intersystem crossing of the host at liquid helium temperatures. At a slightly raised temperature, the triplet excitons are found to transfer efficiently to impurities in the host matrix. With a high doping level of perylene-d12 in very pure dibenzothiophene, most of the triplet excitons found their way to perylene-d12, which resulted in a detectable phosphorescence signal. The triplet state of perylene-d12 is found to be around 784.2 nm (air) or 12,756 cm^{-1} (vacuum) for the main spectroscopic site.

3.1. INTRODUCTION

3.1.1. SCHEME FOR PHOSPHORESCENCE DETECTION

In the previous chapter I introduced the new host/guest system of perylene-d12 in a dibenzothiophene crystal. In this chapter, I will continue with this matrix and report on the triplet state energy. As discussed in the previous chapter, interesting triplet dynamics are observed for this system in the form of reverse intersystem crossing (rISC), acting as a separate pathway for the depopulation of the triplet state. However, these particular dynamics could make it difficult to detect phosphorescence from intersystem crossing from the singlet excited state S_1 to the triplet state T_1, as many triplets could be lost by rISC. Fortunately, the excitation scheme that we have in mind, shown in Figure 3.1, avoids this depletion channel by exciting the host molecules, rather than the guest molecule itself.

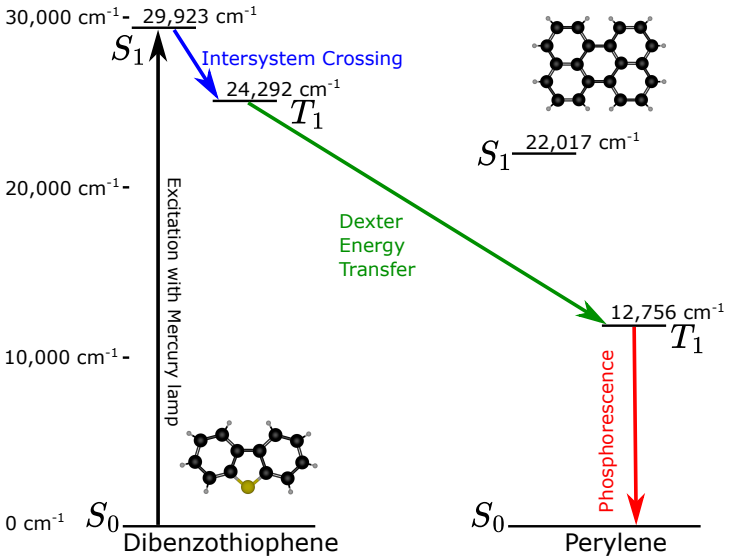

Figure 3.1.: Energy level scheme of perylene-d12 in dibenzothiophene. The energy levels of dibenzothiophene are known from the literature[1] The $S_0 - S_1$ energy gap of perylene-d12 was derived from the emission spectrum in Figure 2.4 of Chapter 2 and the $S_0 - T_1$ energy gap is derived from the phosphorescence spectrum in the present chapter. The excitation scheme relies on a UV excitation (< 334 nm) of the singlet excited state of dibenzothiophene, followed by an intersystem crossing to the triplet state of dibenzothiophene. The excitonic energy may then be transferred to perylene through Dexter energy transfer, where upon the excited triplet of perylene may release a phosphorescence photon.

The excited singlets in the host may decay back to the ground state or form triplets by intersystem crossing (ISC). The ISC rate in dibenzothiophene was found to be

enhanced, likely due to a heavy-atom effect of the central sulfur atom and possibly helped by the relatively small $S_1 - T_1$ energy gap (about 5,632 cm^{-1}). For this reason, dibenzothiophene and related compounds have for instance been used in complexes to achieve efficient room-temperature phosphorescence.[2] After the formation of triplets, the triplets may be transferred by a Dexter energy exchange[3] to the perylene molecule. The Dexter energy transfer decays exponentially with the distance between the perylene and dibenzothiophene molecule, due to its dependence on wavefunction overlap. Due to the very large gap between T_1 of dibenzothiophene and T_1 of perylene, found to be around 11,536 cm^{-1}, it is hard to predict whether this process will actually happen efficiently.

3.2. EXPERIMENTAL

3.2.1. PHOSPHOROSCOPE SETUP

As phosphorescence is a significantly weaker signal than fluorescence, the two signals have to be separated to avoid that fluorescence would saturate the spectrum. Fluorescence is typically very short lived, for perylene in the order of nanoseconds. The phosphorescence is much longer lived, and for example for perylene the triplet has about a 6 orders of magnitude longer lifetime than the singlet. Hence, imposing a short delay between the excitation signal and the detection signal can allow us to filter out the weak phosphorescence signal out of a very strong fluorescence background. The setup (usually called a phosphoroscope, see Figure 3.4) we built to this goal makes use of an optical chopper, which is a rotating wheel with open and closed parts. In our setup we made use of a very simple chopper wheel, that was modified to have a ”pac-man” shape, having an opening of 25% of the surface area, while the rest blocks light. This design is shown in Figure 3.2.

The chopper module consists of a 418F optical chopper and control module from Bentham. This module optically measures the chopper frequency and has an internal circuit to balance the rotation frequency. In the configuration shown in Figure 3.2, the excitation and detection beam are positioned at each side of the chopper. With both beams at the same height, the excitation and detection windows are delayed by a fourth of a rotation cycle. Also, the duration of the excitation and detection windows are a fourth of a rotation cycle.

For the excitation we made use of a 100 W (electrical power) mercury lamp (Newport, 6281) that is fixed in a lamp housing (Oriel, 68810) and powered by a supply unit (Newport, 69911). The old lamp was replaced by a new one to make sure the UV part of the spectrum was not degraded. The lamp housing collects and collimates the light from the arc lamp using a concave mirror and collimation lenses at the output. The light intensity was measured in the 440-460 nm region using a power meter and indicated an integrated intensity of 2.5 mW. Unfortunately, the power meter could not measure UV, but the light could easily be seen as blue fluorescence from white paper. To separate the UV light from the rest of the spectrum, we used a FSR-U340 filter that has the best transmission below 340 nm. However, the filter transmission already starts to decay below 300 nm. The spectrum of the mercury lamp, as transmitted by the filter, is shown

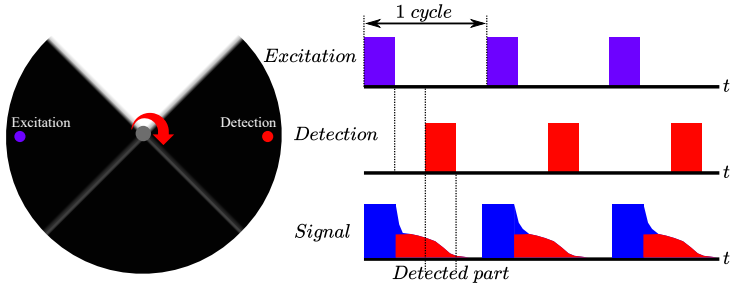

Figure 3.2.: Schematic of the optical chopper scheme. The excitation and detection beam are located at opposite sides of the chopper, which has an open part over a quarter of its area. The rotating chopper makes sure there is a delay of about ¼ of a full rotation between the excitation and detection windows to remove unwanted short-lived photoluminescence, in particular fluorescence. The excitation and detection cycles are shown in a square wave profile on the right. The signal, shown schematically in blue for fluorescence and red for phosphorescence is strongly exaggerated in terms of timescales, as the fluorescence decays six orders of magnitude faster than the phosphorescence of perylene.

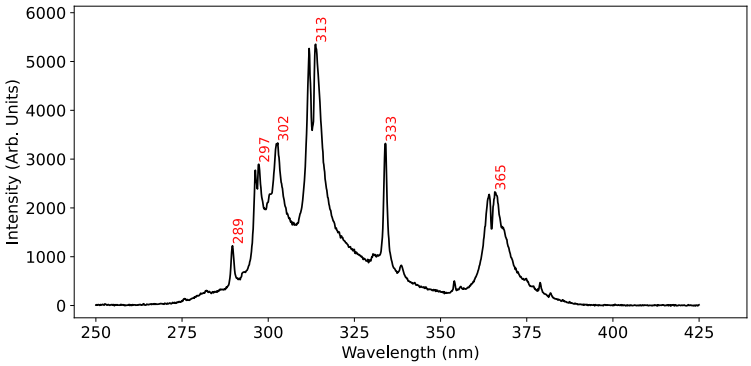

Figure 3.3.: Spectral lines of the mercury lamp that were transmitted by the filter that was used at the excitation side (FSR-U340). All the spectral lines below approximately 334 nm are used for the $S_0 \rightarrow S_1$ transition of dibenzothiophene. The spectral lines above 334 nm could still excite the much weaker $S_0 \rightarrow T_1$ transition of dibenzothiophene.

in Figure 3.3. For an excitation of the host's singlet we need light of a wavelength that is shorter than 334 nm. Thus, the set of spectral lines around 289 nm, 297 nm, 313 nm and 333 nm are likely the most efficient for the excitation of the singlet.

To minimize losses of UV light in the excitation path we made use of aluminum

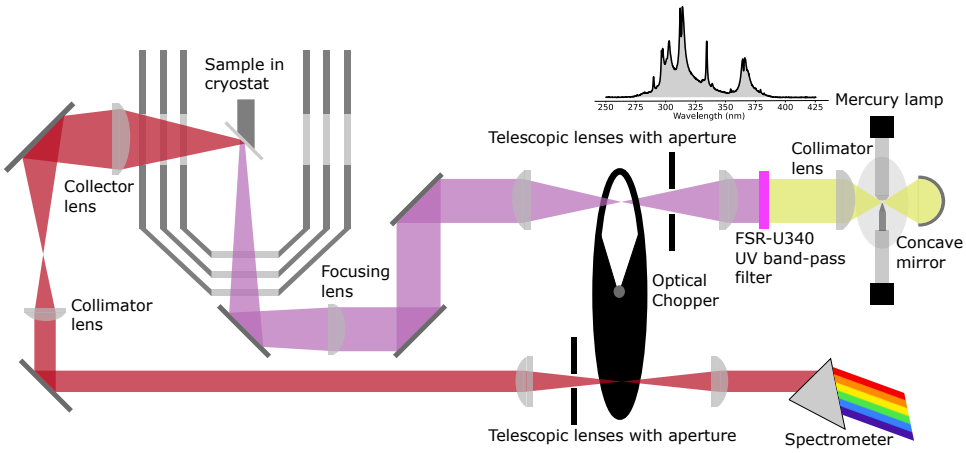

Figure 3.4.: Schematic of the phosphoroscope. Starting from the top right: The collimated light from the mercury arc lamp is filtered to pass the part of the mercury spectrum as shown in Figure 3.3. The UV light is then focused on the chopper, while the beam is cleaned with an aperture. After a focusing lens, the light enters the cryostat from below, passes through the three fused silica windows, and hits the sample with a few mm beam shape. The phosphorescence is collected from the side of the cryostat by a large lens, where further on the emitted light is collimated and again focused onto the chopper and cleaned up by an aperture. Finally, the phosphorescence hits the detector of the spectrometer. Not shown here is the extensive shielding placed between the two light paths. It is important that no light leaks from the excitation path to the detection path, as it can blur weak phosphorescence signals on the spectrometer.

mirrors, which instead of silver has a higher reflectivity in the UV region. Similarly, we used fused-silica lenses to improve UV transmission. A set of two lenses of that type are used in the excitation path. The first lens is used to focus the light on the chopper wheel. The second lens refocuses the diverging beam towards the sample, where the UV light enters the cryostat via fused silica windows. In the detection path we made use of silver mirrors and lenses optimized for the NIR, which is the region where we expect the phosphorescence to be. The light is then focused on the slit of the spectrometer. A slit size of 0.1 mm and a 600 lines/mm grating were the standard settings used for the detection of phosphorescence.

3.3. RESULTS AND DISCUSSION

3.3.1. PHOSPHORESCENCE OF DIBENZOTHIOPHENE

At temperatures of liquid helium and lower, achieved by filling the sample chamber with helium and reducing the pressure, the phosphorescence signal of dibenzothiophene is clearly resolved. A high resolution spectrum of the delayed emission is shown in Figure 3.5. The spectrum is characterized by sharp lines (around 8 ± 2 cm^{-1} in width) and a clearly resolved vibronic structure, only weakly inhomogeneously broadened. The vibrational fingerprint of this spectrum has been assigned before.[1] The origin of the sharp lines is likely related to emission from isolated defect sites, sometimes called X-traps.[1,4,5] It was reported though that the phosphorescence of high-quality crystals could be observed at temperatures up till 77 K, which was not the case for our crystals. This might be related to the doping of the crystals with perylene-d12, the poorer crystallization due to fast quenching and/or other impurities in the crystal. The poorer quality of our crystals is also reflected by the larger inhomogeneous broadening of the lines in Figure 3.5, which was reported to be around 1.5 cm^{-1} for high-quality crystals.[4] The chemical origin of dibenzothiophene might be also different for the commercial dibenzothiophene that we used. In the literature, the dibenzothiophene was synthesized by a reaction of elemental sulfur with highly-purified biphenyl.[4] This route may avoid the formation of some impurities that we have detected in our samples.

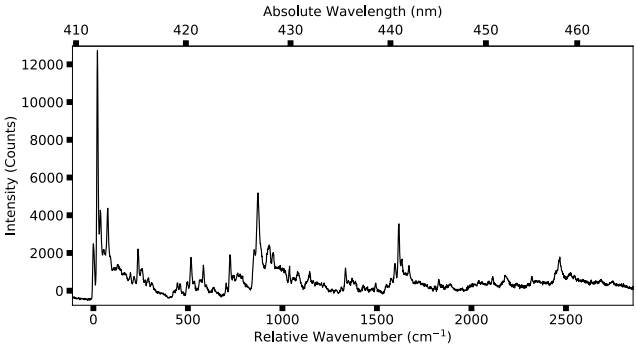

Figure 3.5.: Delayed emission spectrum of dibenzothiophene crystals doped with perylene-d12. The spectrum is recorded at 2 K, where the excited triplet remains trapped on the host molecule. The integration time of the spectrum is 6 minutes, taken with a 0.1 mm slit size and 1200 lines/mm grating. The spectrum is recorded in the second order of the grating to obtain a higher resolution. The first peak in the spectrum was chosen as the origin of the spectrum, with the relative energy of the vibrational peaks indicated in wavenumbers (cm^{-1}).

In addition to the high-resolution settings for the spectrum in Figure 3.5, we also recorded the dibenzothiophene phosphorescence spectrum with the same settings at which we would record the phosphorescence spectrum of perylene. The integrated intensity resulted in a signal on the order of 7.7 million counts per second. This

intensity was more than enough to record the phosphorescence decay over time with a single-photon counter. To record the decay of the phosphorescence signal, the chopper was removed and a mechanical shutter was placed in the excitation path. The measured decay of the phosphorescence signal in Figure 3.6 reveals that the triplet state is very long lived. The phosphorescence decay curve is best fitted with a sum of three exponentials, though two of them have quite close decay times. The short components in the decay curve have lifetimes of 0.24 ± 0.03 s and 0.68 ± 0.01 s, while the long decay has a lifetime of 4.7 ± 0.3 s. The two short lifetimes could be related to the T_x and T_y sublevels of the triplet, while the long lifetime likely belongs to the T_z sublevel. In the literature, the phosphorescence lifetimes of dibenzothiophene were measured to be 0.29 ± 0.02 s for T_x, 0.36 ± 0.02 s for T_y and 9.1 ± 0.8 s for T_z.[4] These individual rates, with two of them very close in time, could be established by microwave-induced delayed phosphorescence (MIDP) experiments, which rely on the saturation of triplet sublevels by inducing a microwave transition to that particular sublevel.[6] However, the close proximity of the T_x and T_y sublevels makes it unlikely that we can distinguish them from the phosphorescence decay and it might be possible that some impurity affects the decay curve, which is measured in the region of 440-460 nm, due to a lack of available filters in the violet region of the visible spectrum.

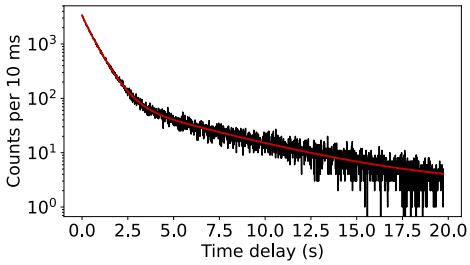

Figure 3.6.: Phosphorescence decay curve of dibenzothiophene crystals at 2 K. The integration time is 10 ms per point, measured in the spectral region determined by a band pass filter between 440-460 nm. The red curve is a fit by a sum of three exponential decays.

3.3.2. PHOSPHORESCENCE OF PERYLENE

Above the temperature of liquid helium, in the region of 4-8 K, the phosphorescence of dibenzothiophene starts to decrease. At this point, the excited triplets will behave as excitons and are able to migrate to deeper traps, which could be perylene molecules or other impurities. In fact, impurities are found to be a limiting factor in some of the experiments. Hence, the concentration of perylene with respect to the concentration of these impurities has to be optimal. Therefore we used a relatively high concentration of perylene-d12 dopant molecules, of around 100 µmol/mol. The location of the dibenzothiophene material in the zone-refining tube was important as well, which is related to the gradients in impurity concentrations along the length of the tube. In

several experiments, the material came from a different position and led to very different results, as each time a different impurity was dominating. Only in the cleanest material were we able to detect the phosphorescence of perylene.

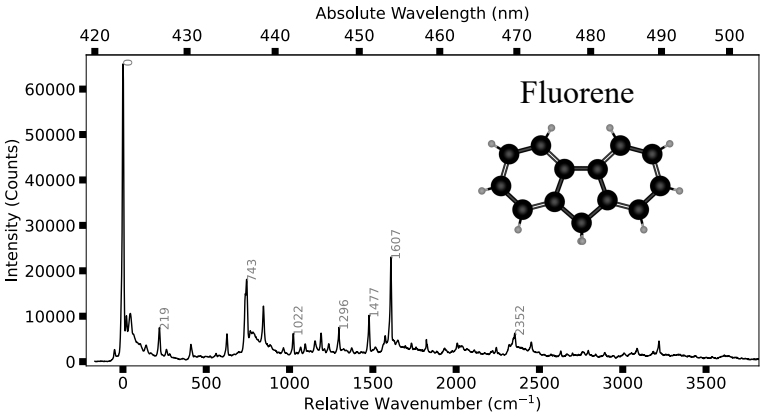

Figure 3.7.: Phosphorescence spectrum of an impurity of dibenzothiophene. Note that the structure of the spectrum is very similar to that of dibenzothiophene. Hence, this is likely a molecule with a related chemical structure. In fact, the vibrational fingerprint matches that of fluorene.[7] The structure of fluorene is shown on the top right. Compared to dibenzothiophene, the central sulfur atom has been replaced with a carbon atom, terminated with two out of plane hydrogen atoms.

A phosphorescence spectrum of an impurity that we could identify is that of fluorene, shown in Figure 3.7. This impurity is not detected in any of the other samples. The dibenzothiophene material that was used in this experiment was extracted closer to the dirty end of the zone-refining tube. Similarly, in other experiments we found two unknown impurities that are phosphorescing. The spectra of these impurities are shown in Figure 3.8. The unidentified compound in Figure 3.8b shows phosphorescence in the most red-shifted region observed so far. The 0-0 zero-phonon line at 672.5 nm indicates that energy was transferred from dibenzothiophene's triplet to the triplet of this compound, bridging a gap of more than 9,400 cm^{-1}. Hence, it may seem possible that the even larger energy gap between the triplet state of dibenzothiophene and the triplet state of perylene-d12 could be crossed as well.

With material from the purest part of the zone-refining tube, we again prepared a high-concentration sample and repeated the measurement. In the phosphorescence spectrum of this sample only an impurity phosphorescing around 475 nm was found (Figure 3.8a), different from the impurities obtained in previous experiments. Although a part of the triplet excitons are lost to this impurity, a relatively good signal could be detected in the expected region of the perylene triplet. The measured spectrum, obtained over the course of 45 minutes, is shown in Figure 3.9. This spectrum was superimposed

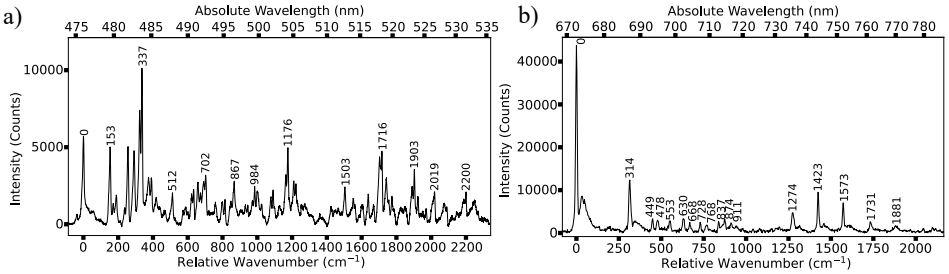

Figure 3.8.: Phosphorescence spectra of unidentified impurities in dibenzothiophene. Panel (a) shows a phosphorescence spectrum of an impurity found in the experiment where we detected perylene-d12 phosphorescence as well. The spectrum is very crowded with lines and might be mixed with another impurity. Panel (b): Apart from perylene-d12, this was the most red-shifted impurity found. The spectrum is different in shape and crowdedness compared to the spectrum of dibenzothiophene in Figure 3.5, the spectrum of fluorene in Figure 3.7 or the spectrum in (a), but resembles more closely a spectrum of a general aromatic compound, without heteroatoms. Unfortunately, the tail of this spectrum stretched all the way into the region of the phosphorescence of perylene-d12, which made this sample useless for the detection of the perylene-d12 triplet energy.

on a strong tail of non-structured delayed luminescence (either phosphorescence or delayed fluorescence from triplet-triplet annihilation). The tail was subtracted by fitting a baseline to it. The origin of the spectrum appears at 784.2 nm or 12,756 cm^{-1}, which is calibrated using a Krypton spectral lamp. The full-width-at-half-maximum of the 0-0 ZPL is around 34 ± 4 cm^{-1}, which is larger than the linewidth detected in the ensemble fluorescence spectrum in Figure 2.4 of Chapter 2. However, the much higher concentration is likely the cause of the broadening. Though the spectral lines correspond with the vibrational fingerprint of perylene-d12, the line shifted by 69 cm^{-1}, which can be observed for all other vibrational peaks as well, is not observed in the fluorescence spectrum. It might be a phonon mode or a different spectral site that was not observed with selective excitation when recording the ensemble fluorescence spectrum. Unlike the selective excitation used for molecules in the fluorescence spectrum, the migration of triplets from the host to perylene-d12 would probably not depend strongly on the energetic position of the perylene-d12 molecules. In section 3.3.3, the possibility of the existence of other sites is studied further and compared to fluorescence spectra.

The location of the triplet state at 12,756 cm^{-1} compares well to the position of the triplet found in anthracene as a host,[8] which was found at 12,844 cm^{-1}. The slight blue-shifted triplet state in anthracene was also observed for the singlet state, which was located at 22,263 cm^{-1}, compared to 22,017 cm^{-1} in dibenzothiophene. The most red-shifted triplet energy was found in the pure crystal of perylene,[9] at 12,372 cm^{-1}.

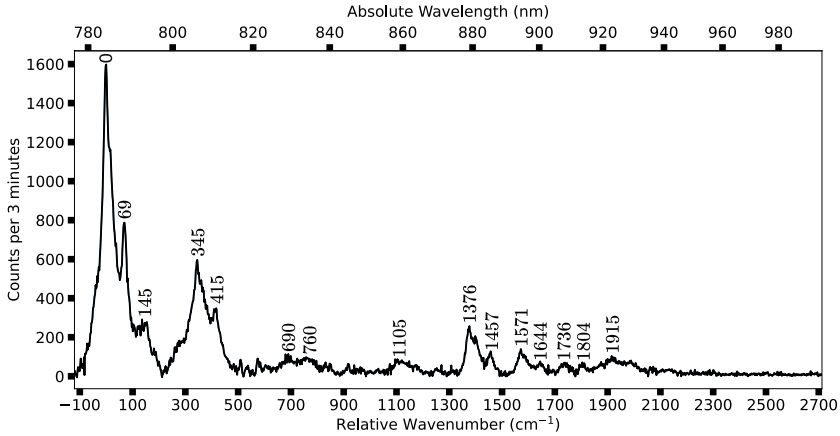

Figure 3.9.: Phosphorescence spectrum of perylene-d12 at a chopper rate of 18 Hz, imposing a delay of 15.6 ms between excitation and detection cycles. The integration time is 45 minutes in total, recorded in two sections, where single spectra are taken at a 3 minute integration time and subsequently merged. The individual spectra are used to remove cosmic rays by substitution. The vibrational fingerprint closely resembles that of the fluorescence spectrum in Figure 3 in Chapter 2, but the lines are much broader due to the high concentration of perylene-d12 and possible mixture of multiple spectroscopic sites (see section 3.3.3).

The integrated intensity of the spectrum gives an average phosphorescence signal of 1000 counts per second. Given that this spectrum is recorded with the same settings as used for estimating the phosphorescence signal of dibenzothiophene we can make a crude estimate of the probability of energy transfer from dibenzothiophene to perylene-d12. However, we need to estimate the quantum yield of phosphorescence as well. Assuming a radiative lifetime $(\gamma_{31}^{rad.})^{-1}$ in the order of 30 s, which was found to be a good approximation for many polyaromatic hydrocarbons,[10,11] we can estimate a quantum yield ϕ_{ph} through the following way:

$$\phi_{ph} = \frac{\gamma_{31}^{rad.}}{\gamma_{31}}. \tag{3.1}$$

Here the rate γ_{31} is the depopulation rate of the triplet state. From the phosphorescence decay of dibenzothiophene in Figure 3.65 we can estimate that for the T_x and T_y state, the triplet depopulation rates will likely be in the order of 2-4 s^{-1} and for the T_z state in the order of 0.2 s^{-1}. This results in an estimated phosphorescence quantum yield of 0.8-1.6 % for the T_x and T_y state and about 16 % for the T_z state. These estimates do not differ much from the reported phosphorescence quantum yield at room temperature for dibenzothiophene, which was found to be in the order of 2-3 %.[12] Similarly, for perylene we estimate a phosphorescence quantum yield of 0.03 % for the T_{xy} sublevels

and 0.2 % for the T_z sublevel. Given that we have phosphorescence quantum yields for perylene and dibenzothiophene, we can estimate the probability for energy transfer by:

$$k_{dbt \to pr} = \frac{\phi_{dbt}}{\phi_{pr}} \frac{N_{pr}}{N_{dbt}} \approx 1\%, \tag{3.2}$$

where N_{dbt} and N_{pr} are the detected phosphorescence signals for respectively dibenzothiophene and perylene. The calculated rate is relatively high, considering that most triplets end up in impurities that are contributing to the strong background in the phosphorescence spectrum and to a structured spectrum at shorter wavelengths, shown in Figure 3.8a. A possible explanation is that not merely the T_1 of perylene is involved in the transfer, but possibly also the T_2 state. A theoretical study of the electronic levels of perylene found that the T_2 state is about 0.2 eV above the singlet excited state S_1.[13] For perylene in dibenzothiophene this would mean that the T_2 state could be located around 23,600 cm^{-1}, which is just below the T_1 state of dibenzothiophene and therefore could provide an additional channel for Dexter energy transfer between dibenzothiophene and perylene (see diagram in Figure 3.10).

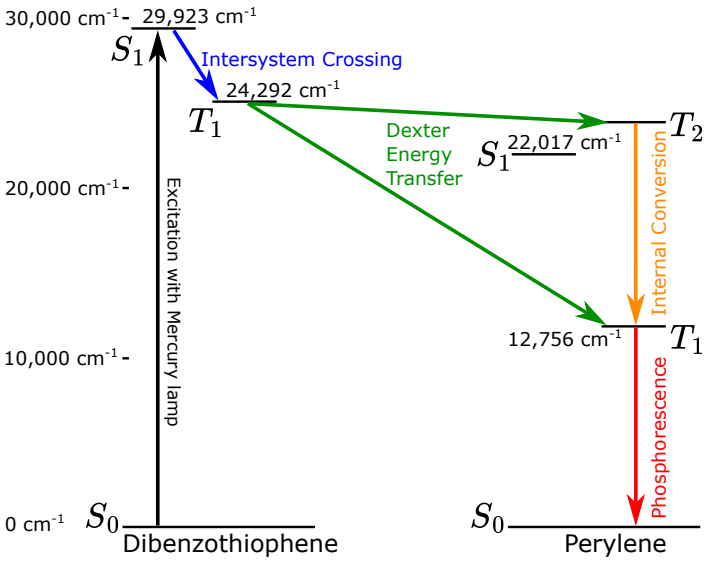

Figure 3.10.: The literature reports[13] that there might be a second triplet excited state T_2 of perylene, which is only 0.2 eV higher in energy than the singlet excited state S_1 of perylene. The energy of T_2 would therefore be slightly lower than T_1 of dibenzothiophene and therefore T_2 of perylene may participate in the energy transfer between dibenzothiophene and perylene.

We also attempted to measure a phosphorescence decay of the spectral region around 780 nm, but the strong background made it difficult to separate the part that can be attributed to perylene-d12. Therefore, we tried to estimate the phosphorescence decay by varying the chopper rate and measuring the integrated intensity of the

phosphorescence spectrum. Based on the chopper frequency we measure the area under the phosphorescence decay curve, which can be derived by integration:[14]

$$N_{pr} = \int_{\frac{1}{4}C}^{\frac{1}{2}C} \sum_{i=1}^{n} A_i e^{-\frac{t}{\tau_i}} dt = f \sum_{i=1}^{n} \frac{A_i \tau_i (e^{\frac{1/4}{f\tau_i}} - 1)}{e^{\frac{1/2}{f\tau_i}}}, \tag{3.3}$$

where f is the chopper frequency, C the period and the sum constitutes the individual exponential decays with characteristic times τ_i and amplitude A_i.

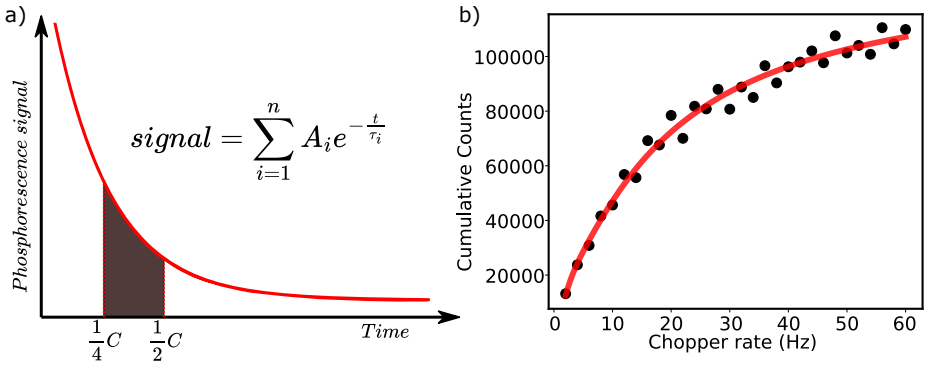

Figure 3.11.: Panel (a) shows a schematic representation of the measured integrated intensity of the exponential decay of phosphorescence in terms of the time per cycle. At an increased chopper rate the integrated area moves to the left. In steady state, the decay curve is represented by the shown formula. Panel (b) shows the integrated intensity of perylene-d12 phosphorescence measured in a single spectrum at various chopper rates. The integration time per point is 120 seconds and the line is a fit of the data to equation 3.3. The best fit is obtained by a sum of two exponential decays.

The two-component fit results in phosphorescence lifetimes of 18 ± 4 ms and 144 ± 58 ms. This is significantly longer than what we find in single-molecule experiments (see Chapter 2): 8.5 ± 0.4 ms and 64 ± 12 ms. However, the uncertainty of the fit in Figure 3.11b is much more significant. In addition, each data point is extracted out of a recorded spectrum, which is superimposed on a strong phosphorescence background with its own time characteristics. By varying some parameters in the isolation of the perylene phosphorescence spectrum from the large background, it was observed that the fit is strongly affected by the value of the points at low chopper rates. These data points are also more uncertain due to the weak signal in the spectra. However, it might be possible that there is some characteristic time delay between the formation of triplet excitons in dibenzothiophene and their migration to perylene-d12. Despite the uncertainty of the phosphorescence lifetimes, the approximate ratio of the two lifetimes does match well with the ratio found in single-molecule experiments.

3.3.3. POSSIBLE EXISTENCE OF MULTIPLE SITES

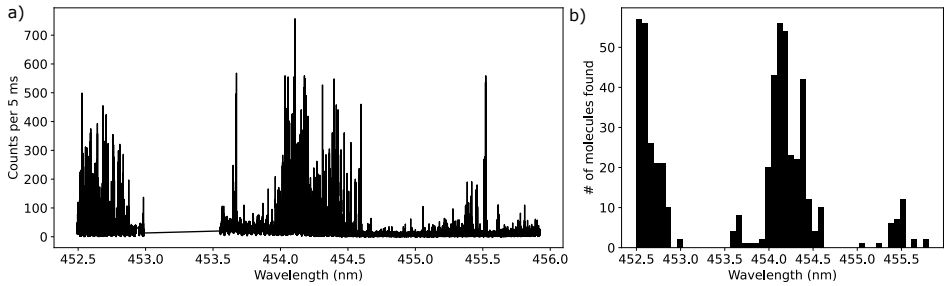

Figure 3.12.: Panel (a) shows a 6 MHz resolution broad range excitation spectrum of a single diffraction-limited focal area in a dibenzothiophene crystal doped with a low concentration of perylene-d12. The scan has a gap around 453 and 453.5 nm, while the rest was recorded. All the peaks are signatures of fluorescence from single molecules and obvious clustering into specific sites is present. Panel (b) shows the average number of molecules detected in a bin of size of 0.07 nm. A total number of 527 molecules are identified.

Although the ensemble fluorescence spectrum in Figure 2.4 of Chapter 2 does not reveal the existence of other spectroscopic sites, the peaks in the phosphorescence spectrum in Figure 3.9, unaccounted for by vibrations (such as the one at 69 cm^{-1}), could be a signature of other spectroscopic sites. Therefore, we studied excitation spectra of perylene-d12 in dibenzothiophene in more detail with another laser that was not present during the studies reported in chapter 2. With this laser (Sacher diode laser with tuning range of about 442-447 nm) we had easier control on scanning large spectral ranges, while avoiding manual adjustments that were necessary with the other laser. A large scan from 452.5 nm up to 456 nm, with a gap between 453 and 453.5 nm, reveals that single perylene-d12 molecules are present in a large spectral range. The main site around 454 nm is present in the scan. However, also additional sites around 452.5 nm and 455.5 nm are revealed. Both sites are approximately 70 ± 10 cm^{-1} shifted in energy with respect to the main site's origin, which is very close to the peak at 69 cm^{-1} in the phosphorescence spectrum. Assuming that both the singlet and triplet states would shift by a similar amount of energy for the sites, the 69 cm^{-1} peak could indeed represent another spectroscopic site, possibly the one around 455.5 nm. This site would have a triplet state around 12,687 cm^{-1} (vacuum) or 788.4 nm (air). Alternatively, it could be that the second bump in the phosphorescence spectrum, around 145 cm^{-1} shifted from the main peak, thus at 12,611 cm^{-1} (vacuum) or 793.2 nm (air), is actually the phosphorescence from the red-most site at 455.5 nm. In that case, the main peak could correspond to the site around 452.5 nm, which does show a significant population in the histogram of Figure 3.12b. This has to be considered when looking for the triplet resonances on a single-molecule level.

3.4. CONCLUSION AND OUTLOOK

By excitation of dibenzothiophene's singlet excited state we have shown that there is efficient transfer of triplet excitons, acquired through intersystem crossing in the host, to the perylene-d12 molecules. However, the measurements have shown that the outcome of this experiment depends heavily on the quality of the dibenzothiophene. Only in the purest samples we were able to obtain a clear phosphorescence spectrum of perylene-d12, with a vibrational signature that confirms it. In addition, the phosphorescence spectrum reveals peaks that are not accounted for by vibrational peaks in the fluorescence spectrum. This could point to the existence of multiple spectroscopic sites, which are likely present, as observed in a broad-range excitation spectrum, measured by fluorescence.

The experiments could be refined by obtaining dibenzothiophene from a source that contains less impurities that are difficult to remove by zone-refining, for example by synthesis that already involves less impurities, such as the identified fluorene. In that case, the concentration of perylene-d12 could be significantly reduced in order to suppress inhomogeneous broadening in the spectrum and obtain a clearer phosphorescence spectrum. Moreover, the inhomogeneous broadening could be further reduced by improving the quality of the crystals by using co-sublimation techniques.

The spectroscopic studies on perylene's phosphorescence could be further extended by using microwaves to transfer populations of all the triplet sublevels to any of the single triplet sublevels, while measuring the phosphorescence spectrum as a function of microwave frequency and chopper frequency, based on microwave-induced delayed phosphorescence experiments. This way, changes in the quantum yield of phosphorescence can be measured while the population is transferred between triplet sublevels, as well as the ensemble-averaged zero-field splitting between the sublevels.

REFERENCES

(1) Bree, A.; Zwarich, R. *Spectrochimica Acta Part A: Molecular Spectroscopy* **1971**, *27*, 621–630.

(2) Zhao, W.; Cheung, T. S.; Jiang, N.; Huang, W.; Lam, J. W. Y.; Zhang, X.; He, Z.; Tang, B. Z. *Nature Communications* **2019**, *10*, 1595.

(3) Dexter, D. L. *The Journal of Chemical Physics* **1953**, *21*, 836–850.

(4) Goldacker, W.; Schweitzer, D.; Zimmermann, H. *Chemical Physics* **1979**, *36*, 15–26.

(5) Ostapenko, N. I.; Sugakov, V. I.; Shpak, M. T., *Spectroscopy of Defects in Organic Crystals*; Springer Science & Business Media: 1993.

(6) Schmidt, J.; Veeman, W. S.; van der Waals, J. H. *Chemical Physics Letters* **1969**, *4*, 341–346.

(7) Bree, A.; Zwarich, R. *The Journal of Chemical Physics* **1969**, *51*, 903–912.

(8) Walla, P. J.; Jelezko, F.; Tamarat, P.; Lounis, B.; Orrit, M. *Chemical Physics* **1998**, *233*, 117–125.

(9) Clarke, R. H.; Hochstrasser, R. M. *Journal of Molecular Spectroscopy* **1969**, *32*, 309–319.

(10) Kellogg, R. E.; Bennett, R. G. *The Journal of Chemical Physics* **1964**, *41*, 3042–3045.

(11) Siebrand, W. *The Journal of Chemical Physics* **1967**, *47*, 2411–2422.

(12) Fang, X.; Yan, D. *Science China Chemistry* **2018**, *61*, 397–401.

(13) Giri, G.; Prodhan, S.; Pati, Y. A.; Ramasesha, S. *The Journal of Physical Chemistry A* **2018**, *122*, 8650–8658.

(14) Zhu, Z.; Shu, X. *Optics Letters* **2018**, *43*, 2575–2578.